Momentum distributions in reactions with radioactive beams

C. A. Bertulani*
National Superconducting Cyclotron Laboratory, Michigan State University, East Lansing, Michigan 48824

K. W. McVoy
Physics Department, University of Wisconsin, Madison, Wisconsin 53706
(Received 2 September 1992)

We investigate the longitudinal and transverse momentum distributions of charged fragments originating from reactions with radioactive, neutron-rich beams. It is shown that the width of the narrow peak of the longitudinal momentum distribution is insensitive to the details of the collision and the size of the target nucleus. In contrast, the width of the peripheral region from which transversely moving particles originate is significantly narrowed via absorption of the outgoing neutrons. This diffractively broadens the width of their transverse momentum distribution, in a manner which depends on details of the collision, and so makes the transverse distribution less reliable than the longitudinal one for measuring the size of the original neutron halo.

PACS number(s): 25.60.+v, 25.70.Mn

Fragmentation reactions with secondary beams of radioactive nuclei have shown that the total reaction cross sections and the transverse momentum distribution of the fragments are sensitive to the separation energy of the last neutrons and to the size of the density profile in these nuclei [1]. These two quantities are linked since the "size" of the nucleus is roughly proportional to the inverse of the square root of the separation energy. Using the Goldhaber model for soft fragmentation, the authors of Ref. [1] were able to relate the widths of the narrow peaks in the transverse momentum distributions with the separation energies and sizes of the radioactive nuclei. However, this approach is not free of bias. The interaction of the fragments with the target broadens the narrow peak and makes the extraction of quantitative information about these quantities strongly model dependent and potentially inaccurate.

We show here that a better measure of the interaction size of the radioactive projectile is obtained by the longitudinal momentum distribution of its fragments. It is also shown that the Coulomb and nuclear fragmentation amplitudes have longitudinal momentum distributions with very nearly equal widths. This fact has indeed been verified in a recent experiment at the National Superconducting Cyclotron Laboratory at Michigan State University (NSCL/MSU) [2]. On the other hand, the transverse momentum distributions are substantially broadened by the size and diffuseness of the region of overlap with the target and contain Coulomb and nuclear contributions with different widths. The interpretation of the "wide" (core-neutron) component of the transverse momentum distributions is therefore less straightforward than is that of the longitudinal ones.

In what follows we shall use a simple cluster description of the radioactive nuclei. The conclusions drawn however are of general validity. The cluster model only serves as a guide to obtain a simpler insight into the results. The systems studied experimentally involve reactions of the form

$$a + A \rightarrow b + x + A^* \equiv b + X \,. \tag{1}$$

According to Ref. [3], a spectator model of $a \equiv b + x$ gives the singles spectra of the particle b as

$$\frac{d^2\sigma}{d\Omega_b dE_b} = \rho(E_b)\,\frac{2E_x}{\hbar v_a\, k_x}\int d^2b_x\,|\tilde{\phi}_a(\mathbf{q}_b,\,\mathbf{b}_x)|^2 \times\left[1-|S_{xA}(b_x)|^2\right], \tag{2}$$

where

$$|\tilde{\phi}_a(\mathbf{q}_b,\,\mathbf{b}_x)|^2 = \left|\int d^3r_b\, e^{i\mathbf{q}_b\cdot\mathbf{r}_b}\, S_{bA}(b_b)\,\phi_a(\mathbf{r}_b-\mathbf{r}_x)\right|^2 , \tag{3}$$

The quantity $S_{iA}(b_i)$ is the S matrix for the scattering of cluster i ($i = b,\, x$) from the target A. We obtain it from a complex optical potential by means of the eikonal approximation. For the optical potential we use the "$t\rho\rho$" formalism (see, e.g., Ref. [4]), which is obtained by folding the nuclear densities of the participant nuclei weighted by the nucleon-nucleon scattering cross section, with medium correction effects. We shall here concentrate on reactions involving ^{11}Li, ^{11}Be, and ^{6}He, and compare our results with the measurements of the momentum distributions of the ^{9}Li, ^{10}Be, and ^{4}He fragments, respectively. Thus in the cases of ^{11}Li and ^{6}He, we are assuming the two removed neutrons behave in the projectile as a single cluster, which the collision removes as a unit. The Hartree-Fock densities for these nuclei were taken from Ref. [5], except for the ^{6}He, which was

*On leave of absence from Instituto de Física, Universidade Federal do Rio de Janeiro, 21945 Rio de Janeiro, Brazil.

taken from Ref. [6]. The density distributions of the knocked-out neutrons were taken as the difference between the neutron distributions of the original nuclei and of the observed fragments.

In Eq. (3), ϕ_a represents the cluster wave function for the incoming $a = b + x$ projectile. If one assumes that the fragment b does not interact with the target, i.e., $S_{bA}(b) \equiv 1$, one finds

$$\frac{d^2\sigma}{d\Omega_b dE_b} = \rho(E_b)\, \sigma^R_{xA}\, |\phi_a(\mathbf{q}_b)|^2 , \tag{4}$$

where σ^R_{xA} is the total reaction cross section of fragment x with the target A, and $\phi_a(\mathbf{q}_b)$ is the Fourier transform of $\phi_a(\mathbf{r}_b - \mathbf{r}_x)$ with respect to $\mathbf{q}_b$. The above result is known as the Serber model limit [7]. It tells us that in this approximation the breakup mechanism measures the momentum-space internal wave function of the projectile, so that the singles spectrum of fragment b provides important information about the internal structure of the projectile. This is especially useful for the study of extremely short-lived nuclei in secondary beam reactions.

Unfortunately, the Serber model is only a rough approximation for most cases and the elastic scattering (including absorption) of the fragment b on the target has to be included, leading to an unavoidable broadening of the momentum distributions [8]. The physical origin of this broadening is simple diffraction (i.e., the uncertainty principle), as an examination of Eq. (3) makes clear. For instance, if $S_{bA} \equiv 1$, the Fourier transform given by this equation would be exactly the Fraunhofer diffraction pattern (as a function of $\mathbf{q}_b$) of the "source distribution" $\phi_a(\mathbf{r}_b - \mathbf{r}_x)$. Including the factor $S_{bA}(b_b)$, with $|S_{bA}(b_b)| \leq 1$, effectively decreases the transverse width of the source by eliminating the part that overlaps with the target A, and this will of course broaden the transverse diffraction pattern. A second possible source of transverse broadening is final-state Coulomb deflection, which is not included in Eq. (2).

This broadening makes it harder to extract the internal momentum structure of the projectile. However, since for high energy collisions the S matrix S_{bA} does not depend on the longitudinal coordinate, the longitudinal momentum distribution is expected to be much less altered by the S_{bA} absorption. This can be illustrated by using a separable wave function, e.g., a Gaussian, in which case the longitudinal and transverse parts of the integral in Eq. (2) factorize completely. That is, if we take for the projectile cluster wave function the approximation $\phi_a \propto \exp\{-(\mathbf{r}_b - \mathbf{r}_x)^2\Delta^2\}$, one finds

$$\begin{aligned}\frac{d\sigma}{dq^{(b)}_{//}} = (2\pi)^2 \frac{E_x}{\hbar v_a k_x} \frac{C^2_\Delta}{\Delta^2} \exp\Big\{-\frac{[q^{(b)}_{//}]^2}{2\Delta^2}\Big\} \\ \times \int d^2b_x\, b_x\, \exp\Big\{-2\,\Delta^2\, b_x^2\Big\}\, \Big[1 - |S_{xA}(b_x)|^2\Big] \\ \times \int db_b\, b_b\, \exp\Big\{-2\Delta^2\, b_b^2\Big\}\, I_0\Big(4 b_x b_b \Delta^2\Big) |S_{bA}(b_b)|^2\end{aligned} \tag{5}$$

where the C_Δ is a normalization constant and I_0 a Bessel function. Thus, the dependence on $q^{(b)}_{//}$ is given by a Gaussian function multiplied by a geometrical factor. Therefore, the longitudinal momentum distribution measures the internal momentum function of the projectile and is insensitive to the details of the nuclear interaction. This result is exact for a Gaussian wave function, and is expected to be approximately true in general simply because S_{iA} is independent of the longitudinal coordinate.

Due to their low separation energies, the projectiles near the β-instability line are also easily Coulomb excited or fragmented [9]. The momentum distribution of the fragments will be determined by a matrix element of the form (in the dipole approximation)

$$\mathcal{M}^{(m)}_{if} = \int r\, Y_{1m}(\hat{\mathbf{r}})\, \phi^*_f(\mathbf{r})\, \phi_i(\mathbf{r}) d^3r . \tag{6}$$

The Coulomb fragmentation cross section is given in terms of this matrix element by [9]

$$\frac{d^3\sigma}{d\Omega_x\, d\Omega_b\, dE_b} = \frac{\mu_{bx}}{(2\pi)^3\hbar^2} \frac{k_x\, k_b}{k_a} \sum_m |f_m(\mathbf{q}, \mathbf{Q})|^2 , \tag{7}$$

where

$$f_m(\mathbf{q}, \mathbf{Q}) = \sqrt{\frac{16\pi}{3}} \frac{1}{2^{m/2}} \frac{Z_T e}{\hbar v} \Big(\frac{k_a \omega}{v}\Big) \chi_m(Q, q)\, \mathcal{M}^{(m)}_{if} \tag{8}$$

and

$$\chi_m(Q, q) = \int J_m(Qb)\, K_m\Big(\frac{\omega b}{v}\Big)\, S_{aA}(b)\, b\, db . \tag{9}$$

In the equations above $\mathbf{k}_a = \mathbf{k}_b + \mathbf{k}_x$, $\mathbf{q} = (m_x\mathbf{k}_b - m_b\mathbf{k}_x)/m_a$, $\mathbf{Q} = \mathbf{k}'_a - \mathbf{k}_a$, and $\hbar\omega = B + \hbar^2 q^2/2\mu_{bx}$, where B is the binding energy of the system $b + x$. To obtain the momentum distributions of fragment b we integrate the above equations with the constraint of energy conservation.

We have evaluated the Coulomb cross sections as well as the nuclear cross sections of Eq. (2) using a Yukawa wave function, $\phi \propto e^{-\alpha r}/r$ for the initial cluster, with $\hbar\alpha = 27.8$ MeV/c for ^{11}Li, corresponding to a binding energy of 0.25 MeV for the two valence neutrons. Their final-state wave function was plane waves for the Coulomb breakup and Glauber for the nuclear breakup, as described in Ref. [3].

The longitudinal momentum distribution of ^{9}Li from the fragmentation of ^{11}Li projectiles with 70 MeV/nucleon has recently been measured at the NSCL/MSU using several targets [2]. The data were taken using light and heavy targets, thus probing the relative strengths of the nuclear and the Coulomb interaction on the breakup. We assume for simplicity that the momentum distributions for Be and Nb targets are induced by the nuclear interaction only, while for Ta targets the Coulomb interaction dominates. The distributions are then calculated by the separate use of Eqs. (2) and (7), respectively. The results are shown in Fig. 1, together with the experimental data.

We also repeated the calculations using a Gaussian wave function and found no significant difference in the

distributions if the Gaussian parameter was chosen to be $\hbar\Delta = 20$ MeV/c in the three cases, too. This confirms our statement that the longitudinal momentum distributions are rather independent of the inducing interaction. However, since only a limited amount of data is available up to now, and in view of our simplifying assumptions about the wave functions, we consider our conclusions as qualitative ones. Further experimental and theoretical investigation is clearly needed in order to settle these ideas.

We turn now to the investigation of the transverse momentum distributions. Figure 2 shows the transverse momentum distributions of ^{9}Li, ^{10}Be, and ^{4}He from the breakup of ^{11}Li, ^{11}Be, and ^{6}He projectiles, respectively, incident on carbon at 800 MeV/nucleon. For this target only the nuclear contribution to the break-up needs to be considered. The data are from Ref. [1]. The dotted curves are the result of the Serber model calculation following Eq. (4). The momentum parameters α of the Yukawa were taken as 27.8, 29, and 49.2 MeV/c for ^{11}Li, ^{11}Be, and ^{6}He, respectively, corresponding to binding energies of 0.25, 0.5, and 0.97 MeV, respectively. The dashed curves were obtained using the more correct approach of Eq. (2), with the same values of α.

In the case of ^{11}Li the result of the Serber model agrees with the one obtained for the longitudinal momentum distribution data of NSCL/MSU, since the momentum

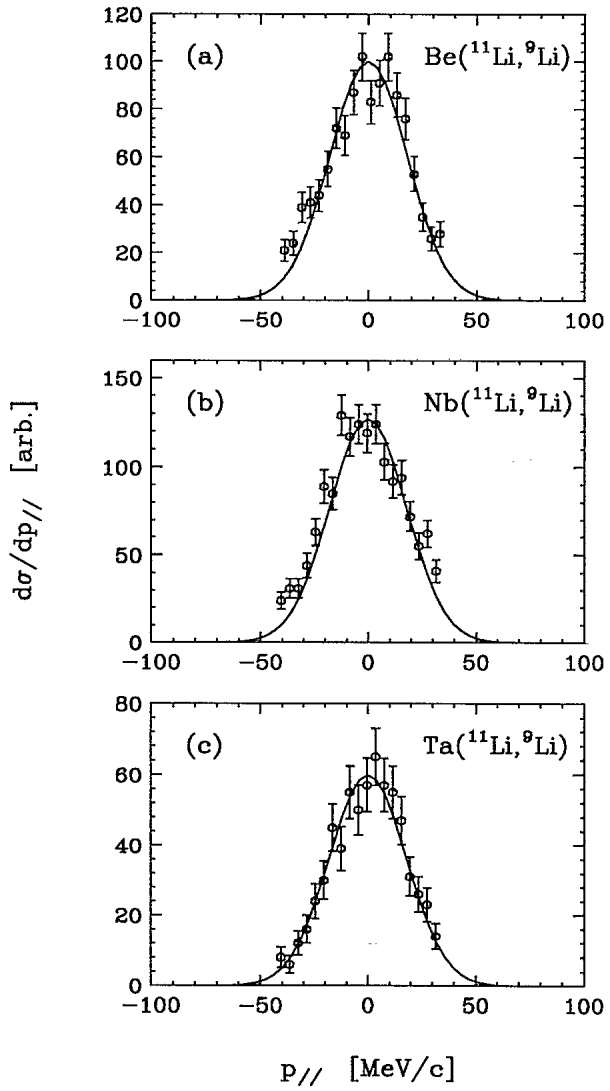

FIG. 1. Longitudinal momentum distributions of ^{9}Li fragments from the breakup of ^{11}Li incident on (a) Be, (b) Nb, and (c) Ta targets, at 70 MeV/nucleon. The data are from Ref. [2], and the curves are from Eqs. (2) and (7), normalized to the data.

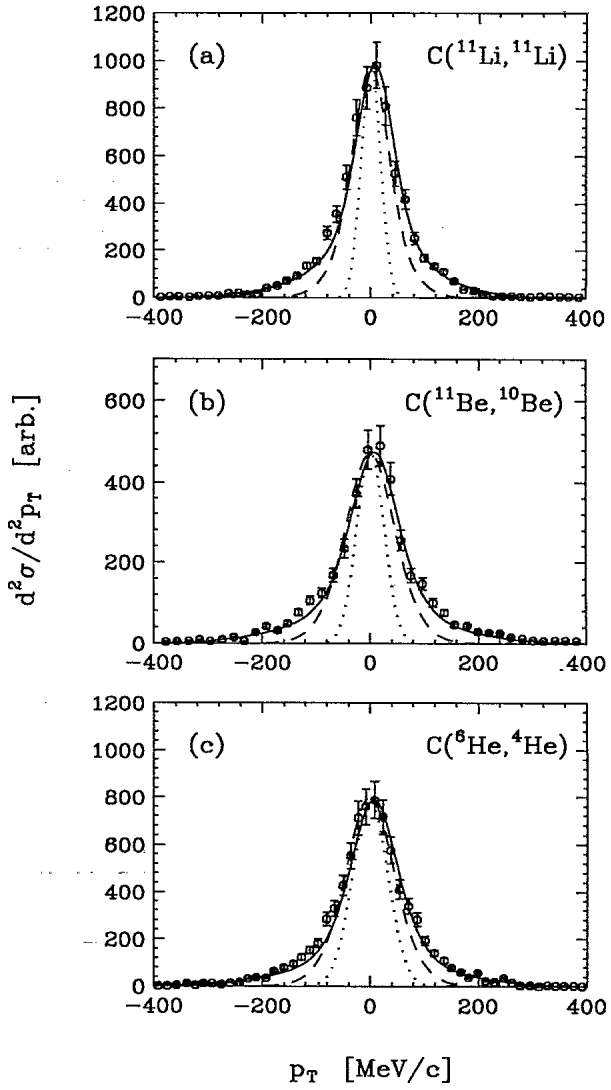

FIG. 2. Transverse momentum distributions of (a) ^{9}Li fragments from the breakup of ^{11}Li, (b) ^{10}Be fragments from the breakup of ^{11}Be and (c) ^{4}He fragments from the breakup of ^{6}He projectiles incident on carbon at 800 MeV/nucleon. The data are from Ref. [1]. The dotted and dashed curves describe halo neutrons only, the dotted curve neglecting final-state neutron interactions with the target, and the dashed curve including them via Eqs. (4) and (2), respectively. The solid curves are 2-Gaussian fits to the data, using widths determined by the binding of the core and halo neutrons of the projectile.

distribution given by this model is isotropic. The interaction of the fragments with the target broadens the peak, and this is displayed by the dashed curves in this figure. However, it is also seen that the wings of the momentum distributions cannot be reproduced by using a single Yukawa parametrization for the ground state wave function. This fact may be due to the simple cluster model picture that we have undertaken. More realistic models are able to describe these wings (wide component) [10], but our analysis is consistent with the idea that the narrow peak is closely related to the separation energy of the halo fragments.

An attempt to explain the wings of the momentum distributions, displayed in Fig. 2 (solid lines), can be made by assuming that also neutrons from the core of the projectile could be removed with appreciable probability [1]. One can assume that the cross sections for the removal of the loosely bound valence neutrons and the more tightly bound from the core add incoherently. The results are shown by the solid lines in Fig. 2. In this calculation we added two results of Eq. (2), for simplicity using Gaussian wave functions $\phi \propto e^{-r^2/\Delta^2}$ for the core and halo neutrons. The values of $\hbar\Delta$ for the halo neutrons were taken as 19.5, 20.6, and 34.7 MeV/c and those for the core neutrons as 55, 92, and 79 MeV/c, for ^{11}Li, ^{11}Be and ^{6}He, respectively. They correspond to the approximate binding energies of valence and core nucleons, respectively. The Hartree-Fock densities for the core nucleons were taken from Refs. [5, 6]. The momentum widths of the "wings" are much wider than the ones cited earlier, and are related to the separation energies of the core neutrons. The contributions of the two Gaussian simulation for the internal wave functions were chosen so as to reproduce as well as possible the experimental data. The good agreement with the experimental data (solid lines in Fig. 2) should therefore be approached with some caution, since any two-Gaussian fit can reproduce the transverse momentum data [1]. The ratio between the two contributions presumably gives roughly the spectroscopic factors for the removal of neutrons from the core and from the halo, respectively. This ratio, $\sigma_{\rm wide}/\sigma_{\rm narrow}$, is suspiciously large, being about 0.4 for the fragmentation of ^{11}Li. It is hard to believe that so many events could arise from the removal of tightly bound neutrons.

Another interesting feature shown in Fig. 2 is a small shift of the peaks with respect to the central position ($q_T = 0$). This shift arises from the phase of the S_i matrices originating in the real part of the potential, but is small and may be neglected.

The above qualitative analysis shows that the longitudinal momentum distribution which results from the fragmentation of weakly-bound light projectiles is rather insensitive to the interaction, and may be a reasonable probe of the internal momentum wave function of the projectile. On the other hand, the transverse momentum distribution depends on the reaction mechanism, and the extraction of definite information about the halo size is not free of bias. One interesting problem to be studied is the extension of the experimental measurements to look for the possible existence of wings in the longitudinal momentum distributions, which do not appear in the data of Ref. [2]. The existence of such wings might provide a more definitive measure of the contribution of more tightly bound nucleons, from the core of the projectiles, which have been assumed to explain the wings of the transverse momentum distribution [1].

We are indebted to N. Orr, B. Sherill, and G. Bertsch for useful discussions. We acknowledge partial support from the U.S. National Science Foundation under Grants PHY-9017077 and PHY-9015255.

[1] T. Kobayashi *et al.*, Phys. Rev. Lett. **60**, 2599 (1988); T. Kobayashi and I. Tanihata, in *Proceedings of the International Symposium on Structure and Reactions of Unstable Nuclei*, Niigata, Japan, 1991, edited by T. Suzuki (World Scientific, Singapore, 1992).
[2] N. Orr *et al.*, Phys. Rev. Lett. **69**, 2050 (1992).
[3] M. S. Hussein and K. W. McVoy, Nucl. Phys. **A445**, 124 (1985).
[4] M.S. Hussein, R.A. Rego, and C.A. Bertulani, Phys. Rep. **201** 279 (1991).
[5] G. Bertsch, B.A. Brown, and H. Sagawa, Phys. Rev. C **39**, 1154 (1989).
[6] Y. Suzuki, Nucl. Phys. **A528**, 395 (1991).
[7] R. Serber, Phys. Rev. **72**, 1008 (1947).
[8] H. Utsunomiya, Phys. Rev. C **41**, 1309 (1990).
[9] C.A. Bertulani and G. Baur, Phys. Rep. **163**, 299 (1988).
[10] M.V. Zhukov *et al.*, Nucl. Phys. **A529**, 53 (1991); *ibid.* **A539**, 177 (1992).